2

Prediction of High-Frequency Ground Motion Parameters Based on Weak Motion Data

Sebastiano D'Amico[1], Aybige Akinci[2], Luca Malagnini[2] and Pauline Galea[1]
[1]*Physics Department, University of Malta, Msida,*
[2]*Istituto Nazionale di Geofisica e Vulcanologia, Rome,*
[1]*Malta*
[2]*Italy*

1. Introduction

Large earthquakes that have occurred in recent years in densely populated areas of the world (e.g. Izmit, Turkey, 17 August 1999; Duzce, Turkey, 12 November 1999; Chi-Chi, Taiwan 20 September 1999, Bhuj, India, 26 January 2001; Sumatra 26 December 2004; Wenchuan, China, May 12, 2008; L'Aquila, Italy, April 6, 2009; Haiti, January 2010 Turkey 2011) have dramatically highlighted the inadequacy of a massive portion of the buildings erected in and around the epicentral areas. For example, the Izmit event was particularly destructive because a large number of buildings were unable to withstand even moderate levels of ground shaking, demonstrating poor construction criteria and, more generally, the inadequacy of the application of building codes for the region. During the L'Aquila earthquake (April, 06, 2009; Mw=6.3) about 300 persons were killed and over 65,000 were left homeless (Akinci and Malagnini, 2009). It was the deadliest Italian earthquake since the 1980, Irpinia earthquake, and initial estimates place the total economic loss at over several billion Euros. Many studies have already been carried out describing the rupture process and the characteristics of local site effects for this earthquake (e.g. D'Amico et al., 2010a; Akinci et al., 2010). It has been observed that many houses were unable to withstand the ground shaking.

Building earthquake-resistant structures and retrofitting old buildings on a national scale may be extremely costly and may represent an economic challenge even for developed western countries, but it is still a very important issue (Rapolla et al., 2008). Planning and design should be based on available national hazard maps, which, in turn, must be produced after a careful calibration of ground motion predictive relationships (Kramer, 1996) for the region.

Consequently, the assessment of seismic hazard is probably the most important contribution of seismology to society. The prediction of the earthquake ground motion has always been of primary interest for seismologists and structural engineers. For engineering purposes it is necessary to describe the ground motion according to certain number of ground motion parameters such as: amplitude, frequency content and duration of the motion. However it is necessary to use more than one of these parameters to adequately characterize a particular ground motion.

Updating existing hazard maps represents one of the highest priorities for seismologists, who contribute by recomputing the ground motion and reducing the related uncertainties. The quantitative estimate of the ground motion is usually obtained through the use of the

so-called predictive relationships (Kramer, 1996), which allow the computation of specific ground-motion parameter as a function of magnitude, distance from the source, and frequency and they should be calibrated in the region of interest. However this is only possible if seismic records of large earthquakes are available for the specific region in order to derive a valid attenuation relationship regressing a large number of strong-motion data (e.g. Campbell and Bozorgnia, 1994; Boore *et al.*, 1993; Ambraseys *et al.*, 1996, Ambraseys and Simpson, 1996; Sabetta and Pugliese, 1987, 1996; Akkar and Bommer 2010). For the Italian region the most used attenuation relationships are those obtained by Sabetta and Pugliese (1987, 1996) regressing a few data recorded for earthquakes in different tectonic and geological environments. It has been shown in several cases that it is often not adequate to reproduce the ground motion in each region of the country using a single model. Furthermore the different crustal properties from region to region play a key role in this kind of studies. However, the attenuation properties of the crust can be evaluated using the background seismicity as suggested by Chouet et al. (1978) and later demonstrated by Raoff et al. (1999) and Malagnini et al (2000a, 2007). In other words, it becomes possible to develop regionally-calibrated attenuation relationships even where strong-motion data are not available. One of the purposes of this work is to describe quantitatively the regional attenuation and source characteristics for constraining the amplitude of strong motion expected from future earthquakes in the area. In this work we describe how to use the background seismicity to perform the analysis (details in Malagnini et. 2000a, 2007). In particular, this chapter describes the procedures and techniques to study the ground motion and will focus on describing both strong motion attenuation relationships and the techniques used to derive the ground motion parameters even when strong ground motion data are not available. We will present the results obtained for different regions of the Italian peninsula, showing that the attenuation property of the crust and of the source can significantly influence the ground motion. In addition, we will show that stochastic finite-fault modeling based on a dynamic frequency approach, coupled with field investigations, confirms to be a reliable and practical method to simulate ground motion records of moderate and large earthquakes especially in regions prone to widespread structural damage.

2. Weak motion data set processing

In general, a large dataset of weak motion data are processed by following the approach described in details by Malagnini *et al*. (2000a, 2007). The advantage of the procedure is that no hypothesis on the functional form of the scaling laws needs to be formulated before the analysis. The method takes into account the duration parameter, as a function of frequency and distance, through the statistical tool called Random Vibration Theory (RVT, see Cartwright & Longuet-Higgins 1956). The latter is used to estimate the peak ground motion of a random time history, given the empirical attenuation parameter, source spectrum and its duration in time. A detailed description of the method and data processing technique are provided in Malagnini *et al*. (2000a, 2007).

Each waveform is visually inspected to eliminate recordings with low signal-to-noise ratios, anomalous glitches, and calibration issues., and seismograms are corrected for the instrument response. The pickings of the P- and S-wave arrivals are also reviewed. Each corrected time series is filtered using bandpass filter at every f_0 constructed as the contribution of two 8-pole Butterworth filters: a low-pass filter and a high-pass filter with corner frequency, respectively, at $\sqrt{2}\, f_0$ and $1/\sqrt{2}\, f_0$.

A general form for a predictive relationship for observed ground motion is (Fig. 1):

$$A_{ij}(\mathrm{f},\mathrm{r_{ij}}) = EXC_i(\mathrm{r_{ref}}, f) + SITE_j(\mathrm{f}) + D(r_{ij}, r_{ref}, \mathrm{f}) \quad (1)$$

where $A_{ij}(f)$ represents the logarithm of peak amplitude of ground-motion velocity at site "j" for the earthquake "i" on each filtered seismogram recorded at the hypocentral distance $r_{ij,}$ $EXC_i(\mathrm{r_{ref}}, f)$ is the excitation term; $SITE_j(f)$ represents the site term and describes the site modification effects; and $D(r_{ref}, r, f)$ is the crustal propagation term and represents an estimate of the average frequency-dependent crustal response for the region. Usually the value of 40 km is chosen for r_{ref}. A piece-wise linear function defined by fixed-distance nodes was used to model the $D(r,\mathrm{r_{ref}},f)$ function. The number of nodes of this piece-wise linear function, and the spacing between the nodes are selected according to the distance distribution of our data. Equation (1) is solved in the time domain, from multiple narrow band-passed signals.

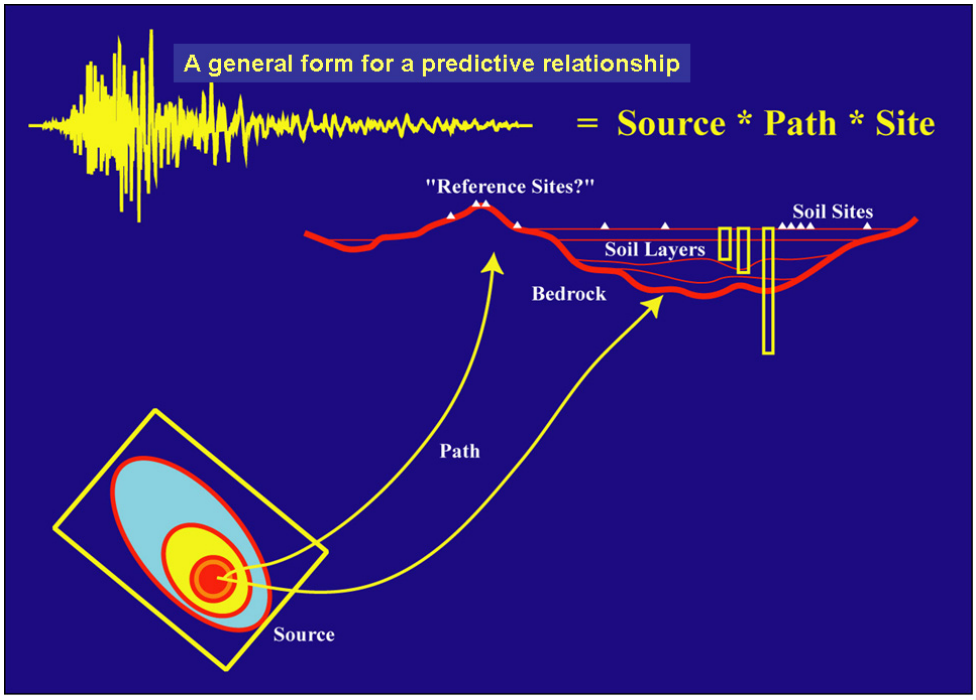

Fig. 1. Schematic representation of a general form for a predictive attenuation relationship.

By using the model equation (1), we can arrange all our observations in a large matrix and then invert to obtain source, path and site terms. According to Malagnini *et al*. (2000a) the regression requires two constraints for stable inversion:

$$D(r_{ij}=r, r_{ref}, f)=0 \quad (2a)$$

$$\Sigma SITE_i\ (f)=0 \quad (2b)$$

The first constraint defines the distance to which the excitation term is projected. The effect of the second one is that common site effects are mapped on the excitation term. During the

inversion the sum of all site terms is forced to zero (relation 2b) for each frequency, so that the source terms represent what would be recorded at the reference hypocentral distance by the average network site. Each individual site term measures the deviation from the mean seismic spectra for each station, which is due to the physical properties of the shallow geology at the recording site or, in some cases, to instrumental calibration.

The duration of ground motion is a function of the fault size and of the dispersion of elastic waves along the path between the source and the seismic station. To make specific predictions for large earthquakes, the duration of the event must be added in the form of a constant term equal to the inverse of the corner frequency. Since no unique definition of the effective duration of the ground motion is possible, we define the effective duration for the ground motion as given by Raoof *et al.* (1999). Then for each seismogram the duration T is determined as the width of the time window that delimits the 5%-75% portion of the seismic energy following the S-wave arrivals.

The functional form for the propagation terms expresses the effects of frequency-dependent geometrical spreading and anelastic attenuation (Aki, 1980), depending, for each frequency, on the average velocity structure along the propagation path and rock's physical properties. Therefore, we obtain the results of the regression at a set of sampling frequencies, and model them by using the following functional form:

$$D(r, r_{ref}, f) = \log[g(r)] - \log[g(r_{ref})] - \frac{\pi f (r - r_{ref})}{\beta Q(f)} \tag{3}$$

where $g(r)$ is the apparent geometrical spreading, β is the shear-wave velocity, and the frequency-dependent attenuation is defined through the quality factor, $Q(f)$, which is defined as

$$Q(f) = Q_0 \left(\frac{f}{f_{ref}} \right)^{\eta} \tag{4}$$

with the reference frequency f_{ref} chosen at 1 Hz. The parameter η defines the frequency dependence of $Q(f)$.

The term: $\log_{10}(D(r, r_{ref}, f))$ is modeled as a piecewise linear function between a number of distance nodes, and assumed to be zero at a reference distance r_{ref}, which defines the excitation term $\log_{10}(EXC_i(r_{ref}, f))$. The r_{ref} is chosen such that mislocations in source depth would not significantly change the reference hypocentral distance. A body-wave-like geometric attenuation and a surface-wave-like decay is used to model the decay of the Fourier amplitudes as a function of distances (Malagnini et al., 2000a)

The source excitation, $EXC_i(r_{ref}, f)$ in equation (1), may be thought of as the average expected level of ground motion at r_{ref} for each earthquake. The observed excitation is related to the actual source spectrum through the expression

$$\mathrm{EXC_i}(\mathrm{r_{ref}}, \mathrm{f}) = \mathrm{s}(\mathrm{f}, \mathrm{M_w})\, \mathrm{g}(\mathrm{r_{ref}})\, \exp[-\pi\, \mathrm{f}\, \mathrm{r_{ref}} / \mathrm{Q}(\mathrm{f})\beta]\{\mathrm{V}(\mathrm{f})\, \exp(-\pi\, \mathrm{f}\, \kappa_o)\}_{\mathrm{avg}} \tag{5}$$

where $s(f,M_w)$ is the source excitation as a function of moment magnitude, $V(f)$ is a frequency-dependent 'regional' site amplification (the average site term of the stations included in Eq. 2b) and κ_0 controls near-surface attenuation at high frequency. The term $[g(r_{ref})\ exp(-\pi f\, r\, /Q(f)\beta)]$ represents the effect of the propagation at the reference distance due to geometrical spreading and crustal attenuation. The term $\{V(f)exp(-\pi f\ \kappa_o)\}_{\mathrm{avg}}$ term

controls the average site modification of the signal spectrum. $V(f)$ represents the average site amplification term relative to hard rock (in the manner of Atkinson & Silva, 1997), and can be calculated from the shallow shear-wave velocity structure near the site (Boore, 1996). κ_o describes the depletion of the high-frequency motion at the site, which may be caused by the local Q(z) structure. The form of $s(f,M_w)$ representing the Fourier velocity spectra is,

$$s\,(f, M_w) = K\,[M_o/4\pi\rho\beta^3]\,(2\pi f)\,S\,(f) \tag{6}$$

where $\log M_o = 1.5(M_w + 6.03)$ (M_0 in Nm) (from Hanks & Kanamori 1979), K = (0.55 2.0 0.707) is a coefficient composed of the effects of the average radiation pattern, free-surface amplifications for vertically incident S waves and the energy partition of initial shear wave amplitude into two horizontal components, M_o is the seismic moment, ρ is the mass density at the source and β is the shear wave velocity at the source (D'Amico et al., 2011b). $S(f)$ is the single-corner source term:

$$S(f) = 1/\,[1 + (f/f_c)^2] \tag{7}$$

where $f_c = 0.49\beta(\Delta\sigma/M_o)^{1/3}$. Here the corner frequency f_c is determined from the spectra and is related to the stress drop, $\Delta\sigma$ (Pa), seismic moment, M_o (N-m) and the shear wave velocity β (m s^{-1}). The constant 0.49 depends on the type of model spectra and the geometry of the source.

In order to model the excitation term, we use Brune's (1970, 1971) ω^2 source model, which describes the spectrum of shear radiation in terms of stress drop and moment magnitude. The average stress parameter required to best reproduce the observed propagation-corrected source spectra for the larger earthquakes in the data is adjusted using a trial-and-error procedure. In order to properly calibrate the $\Delta\sigma$, and k_0 the scaling relations must be constrained by using moment magnitudes derived from regional moment tensor inversion, both for small and moderate earthquakes (e.g. D'Amico et al. 2010b, D'Amico et al 2011a). In general, a tradeoff exists between the stress parameter and κ_0. κ_0 governs the high-frequency decay of the theoretical excitation terms, as well as the $\Delta\sigma$, which affects the radiated spectra beyond their corner frequencies. In the frequency band of our interest, however, the effect of the stress parameter is strongest for the largest earthquakes, while κ_0 completely controls the behavior of the small earthquakes at high frequency. For this reason, it is necessary first to find estimates of the high frequency parameter, k_0, by examining the spectra of small events, and then, knowing k_0, of the stress parameter of the larger events. During the inversion the sum of all site terms is forced to zero for each frequency. This constraint represents what would be recorded at the reference hypocentral distance by the average network site. The site term measures the deviation from the mean seismic spectra for each station, which is due to the physical properties of the shallow geology at the recording site.

The methodology described above for determining the attenuation properties has been successfully applied in different part of the world: California (Raoof et al. 1999; Malagnini et al. 2007), northwestern United States (Herrmann and Dutt, 1999; Jeon and Herrmann 2004), central United States (Herrmann and Malagnini, 1996), Mexico (Ortega et al., 2003), Greece and Crete (Pino et al., 2001), Italy (Malagnini et al., 2000a, 2002; Malagnini and Herrmann 2000; Morasca et al. 2006; Scognamiglio et al. 2005), Central Europe (Malagnini et al, 2000b, Bay et al. 2003), Turkey (Akinci et al., 2001, 2006), India (Bodin et al., 2004). For example, comparisons can be done among different Italian regions in which this kind of studies have been conducted. It has been found that the western Alps (Morasca *et al.*, 2006), eastern Alps (Malagnini *et al.*, 2002), Southern Appenines, central Italy (Malagnini et al 2000a) and eastern Sicily (Scognaniglio et al 2005) have different characteristics for the attenuation parameters. For instance the crustal wave propagation in eastern Sicily is more efficient than

in other Italian regions. The combination of the geometrical spreading function and the parameter $Q(f)$ is strictly related to the crustal characteristics. Figure 2 reports the attenuation values for each region of Italy for a comparison.

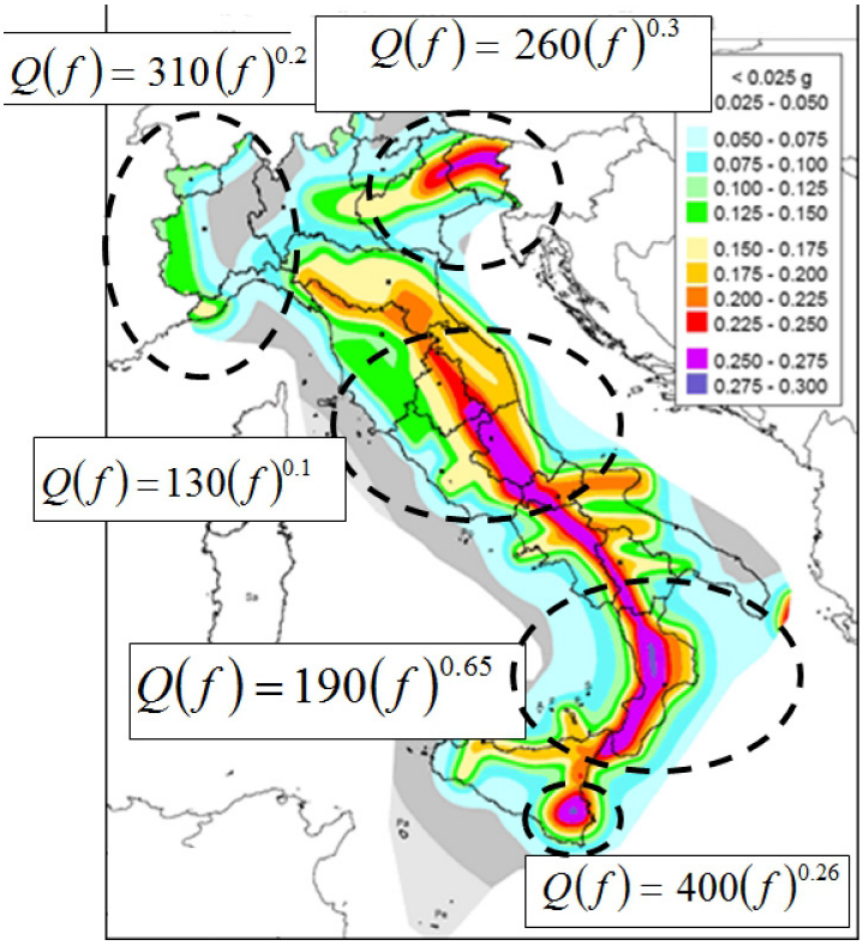

Fig. 2. Attenuation values for different Italian regions: western Alps (Morasca *et al.*, 2006), eastern Alps (Malagnini *et al.*, 2002), Southern Appenines (D'Amico et al. 2011d), central Italy (Malagnini et al 2000a) and eastern Sicily (Scognaniglio et al 2005). The values are plotted on the Italian seismic hazard map please refer to the following website for further details http://zonesismiche.mi.ingv.it ("Mappa di pericolosità sismica del territorio nazionale".

3. Prediction of ground motion parameters

The estimation of ground motion for a particular region and also site-specific investigation is essential for the design of engineered structures. Estimates of expected ground motion at a given distance from an earthquake of a given magnitude are fundamental inputs to

earthquake hazard assessments. The determination of seismic design criteria for engineered structures depends upon reproducible estimates of the expected lifetime of the structures. There are also several site classification schemes used in different papers ranging from qualitative description of the near surface material to very quantitative definitions based on shear wave velocities. In order to predict the expected ground motion parameters (e.g. in terms of peak ground acceleration (PGA) and peak ground velocity (PGV) as a function of distance and magnitude we used a stochastic approach. We performed the task by using two widely used computer codes; for point-source model, SMSIM and for extended-source model, EXSIM that is originally developed by Boore (1996, 2003) and Motazedian & Atkinson (2005) & Boore (2009), respectively. During the SMSIM point-source simulations we did not use any information about fault geometry and rupture properties. In general, the simulations are carried out by using the regional propagation parameters derived as described above and, for the EXSIM simulations, having rectangular faults having length and width proportional to the moment magnitude according to the relationship proposed by Wells and Coppersmith (1994). Each fault is assigned with a random slip distribution, if known, otherwise it is reasonable to assume a random slip distribution if we do not have any constraint on the slip distribution. It has been shown that only the gross features of slip distribution on a fault plane that do not diverge significantly from the average value of slip may be reliable; all other complexities could be extremely uncertain (Beresnev and Atkinson, 2002). During each simulation the fault plane is discretized into several subfaults. Site effects at a specific station are very important and may be used for engineering purpose to define the regional predictive law and the seismic hazard. In the simulations in order to consider different site conditions, we will refer to the NEHRP classification (BSSC, 1994). Figures 3, 4, 5, and 6 shows several examples of stochastic simulations (both using SMSIM and EXSIM) carried out in different parts of the globe. Figure 3 shows a ccomparison between observed and simulated (a) PGA and (b) PGV obtained for the large and destructive Chi-Chi (Taiwan) event that occurred on 20th September 1999. The simulation values are obtained using the EXSIM computer codes. The PGA and PGV simulated values were estimated for an earthquake of $\mathbf{M_w}$ 7.6 using the parameters derived by D'Amico et al. (2011b), and the proposed fault geometry by Ma et al. (2001). The grey symbols represent the observed data of the Chi-Chi earthquake (http://www.cwb.gov.tw). Predictions obtained using Akkar & Bommer (2010), Boore & Atkinson (2008) and Campbell & Bozorgnia (2008) are also shown.

Figure 4 shows the observed PGA and PGV for the L'Aquila (6 April 2009) main shock (Mw= 6.2, D'Amico et al. 2011d). The figures show the theoretical predictions based on the results by Malagnini et al . 2011 for the Generic Rock Site (Boore & Joyner 1997), and from the strongmotion relationships by Sabetta & Pugliese (1996). Predictions are given in terms of medians values $\pm 1\sigma$. Predictions by Akinci *et al.* (2010), computed using the ground motion model developed by Malagnini *et al.* (2008), are only slightly different from the ones obtained in this study, and fit quite well the recorded strong motion data up to a distance of 200 km (Malagnini et al. 2011).

Figure 5 and 6 report the ground motion simulated parameter in terms of PGA and PGV, for the island of Malta due to the possible activation of two active faults located (i) on the Hyblean-Maltese Escarpment, at an epicentral distance of 140 km and (ii) about 20 km south of Malta (D'amico et al. 2011c). In particular for the fault on the Hyblean-Maltese Escarpment we simulated the possible ground motion parameters for four earthquakes of different moment magnitude. It is worth noting on these figures that peak ground accelerations close to $0.1g$ would be generated on Class B and C sites from a magnitude 7.6 event on the Malta escarpment. Such an event is comparable to the 1693 and the 1169 events

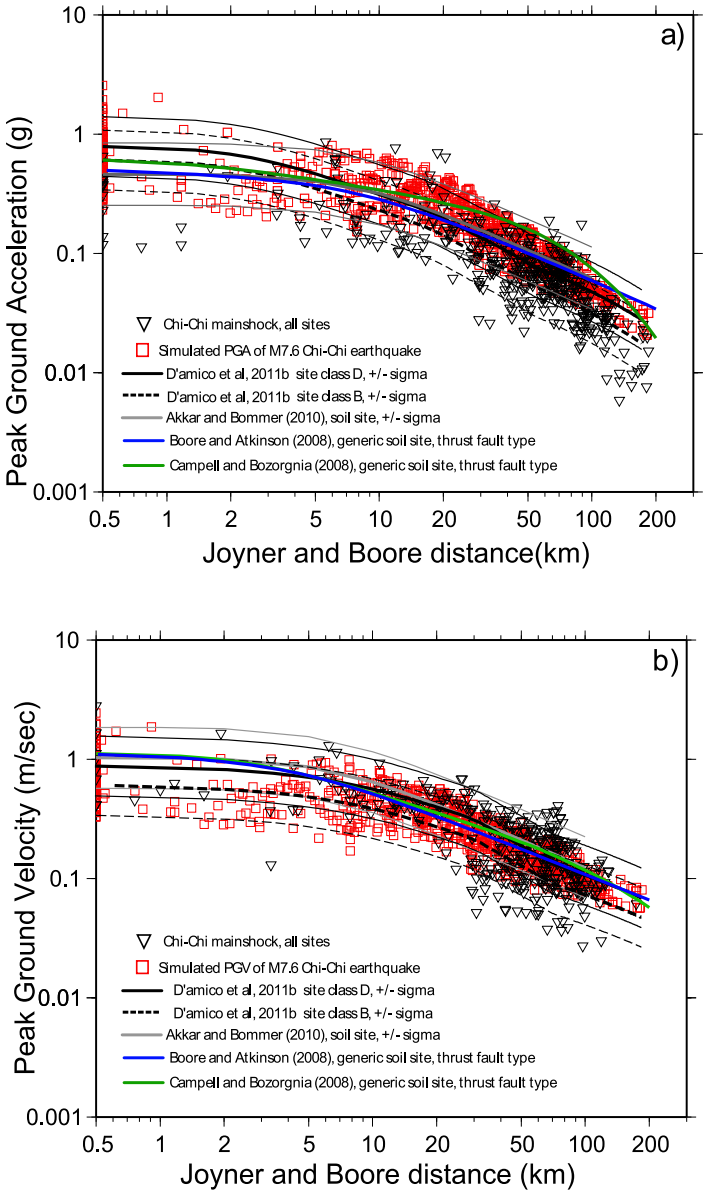

Fig. 3. Comparisons between observed and simulated (a) PGA and (b) PGV. The simulation values are obtained using the EXSIM computer codes. The PGA and PGV simulated values were estimated for an earthquake of $\mathbf{M_w}$ 7.6 using the parameters derived by D'Amico et al. 2011b, and the proposed fault geometry by Ma et al. (2001). The grey symbols represent the observed data of the Chi-Chi earthquake (http://www.cwb.gov.tw). Predictions obtained using Akkar & Bommer (2010), Boore & Atkinson (2008) and Campbell & Bozorgnia (2008) are also shown.

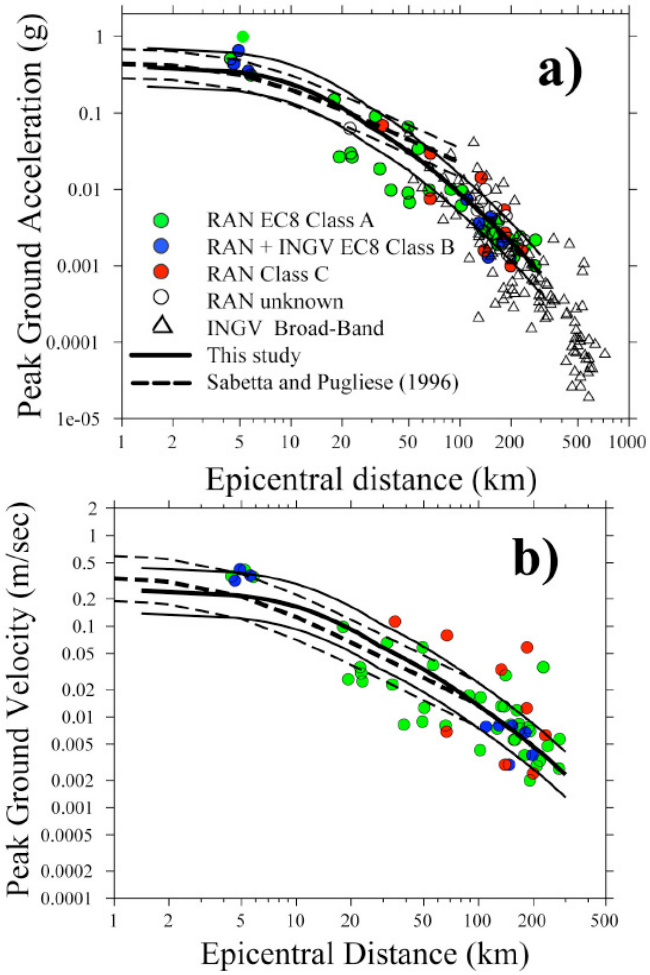

Fig. 4. (a) Predictions of peak ground acceleration (PGA) for the L'Aquila main shock (*M*w 6.15) and comparison with the observed data (Malagnini et al. 2011). Solid lines refer to the predictions calculated in this study (median $\pm$ 1σ), whereas dashed lines refer to Sabetta Pugliese (1996, SP96 in the figure). (b) Same as in frame (a) but for peak ground velocity (PGV). The agreement of the ground motion model presented in his study with the observations gathered during the main shock allow an objective judgment of the model's performance. Observed PGAs and PGVs are characterized, when available, by their Eurocode 8 class (symbols in colours).

on the same fault (Azzaro and Barbano, 2000). Because of the inherent brittleness, lack of ductility and lack of tensile strength of unreinforced masonry buildings (URM), it is expected that even such accelerations could cause significant damage in these buildings (Hess, 2008). It is also observed that a magnitude 5 event on the active fault zone immediately south of Malta would produce similar PGA/PGV values as the above event, albeit the frequency content would be different. Such a magnitude is rare on the Sicily

Channel faults but approximate calculations based on radius of perceptibility indicate that they have occurred on at least one occasion (1911) in the past century.

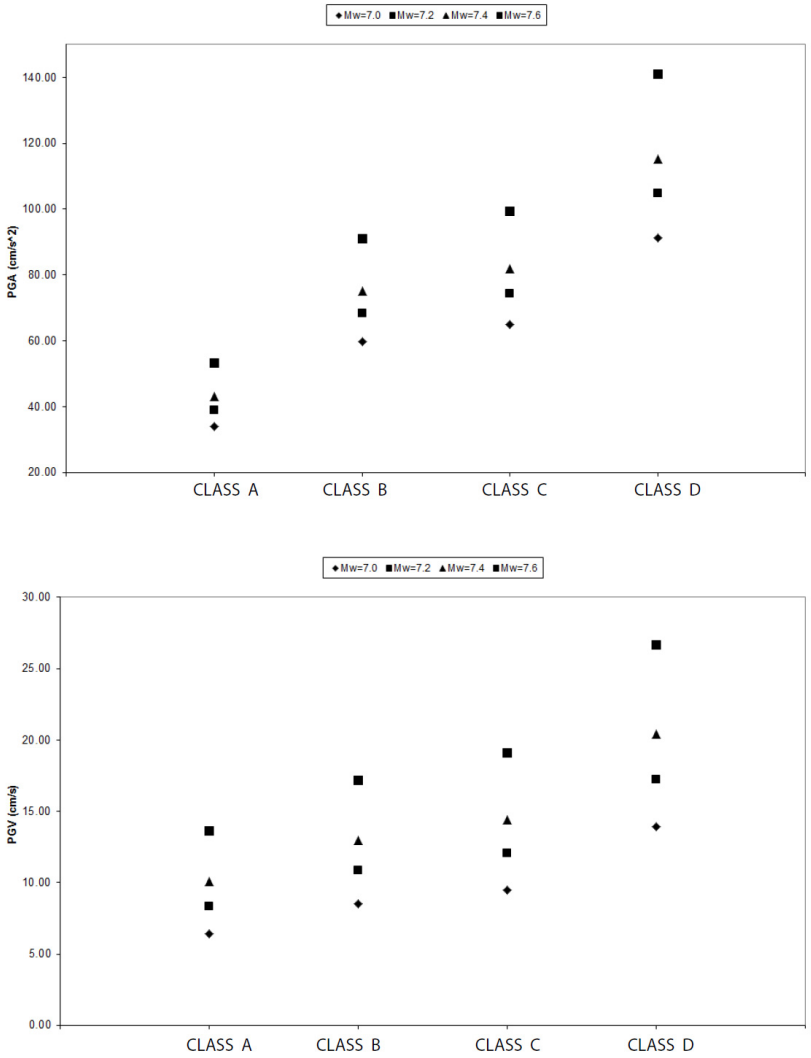

Fig. 5. Predictions of Peak Ground Acceleration (PGA) and Peak Ground Velocity (PGV) for earthquakes of different magnitudes located on the Malta escarpment, at 140km distance. The simulation values are obtained using the EXSIM computer codes. The PGA and PGV simulated values were estimated for an earthquake of Mw 7.0, 7.2, 7.4, and 7.6 (see D'Amico et al. 2011c for details. Each site class is characterized by the average Shear-Wave Velocity over the Upper 30 m (Vs30). In particular, for the class A Vs30~2900m/s; class B Vs30~620m/s; class C Vs30~520m/s; class D Vs30=255m/s (Boore and Joyner, 1997). Preliminary investigations of shallow crustal properties in the Malta area indicate a high variability of soil categories (Panzera *et al* 2011) and therefore the simulations were carried out for each site class.

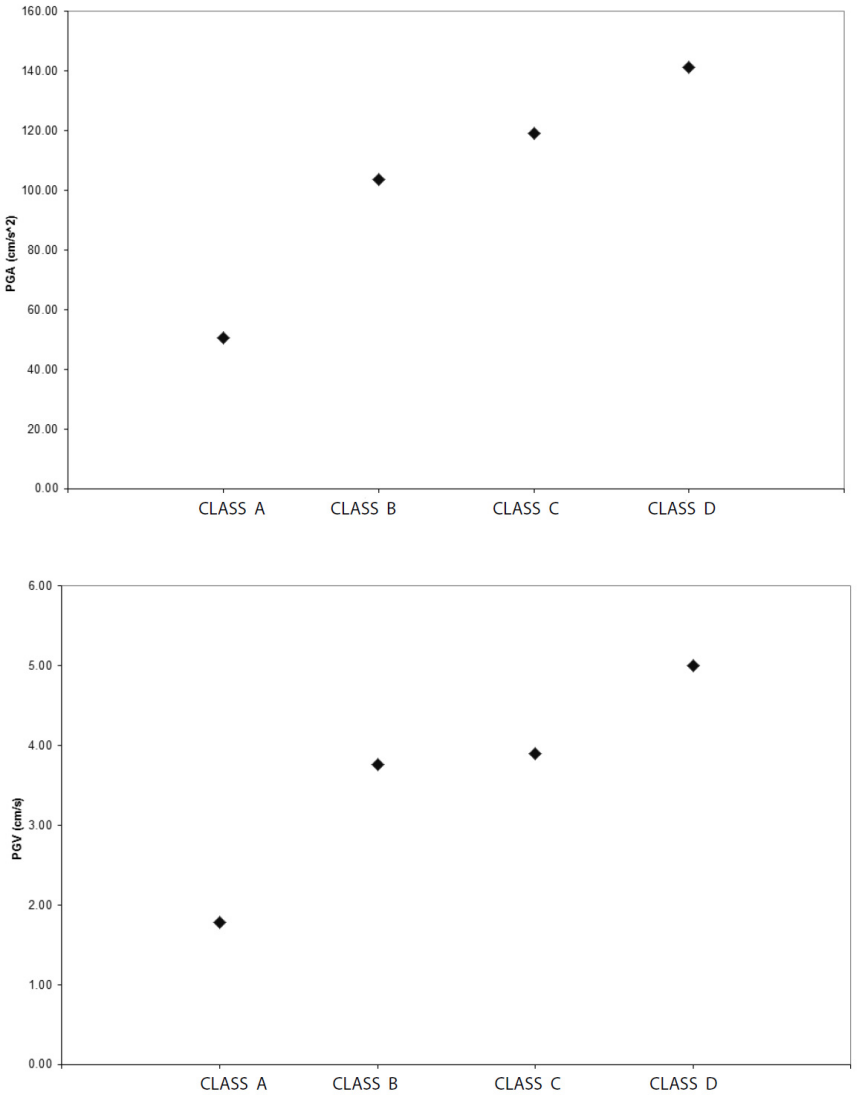

Fig. 6. Predictions of Peak Ground Acceleration (PGA) and Peak Ground Velocity (PGV) for a magnitude 5 earthquake located at about 20 km south of Malta. See caption of Figure 5 for details.

4. Comparison between simulated ground motions for different moment magnitude events from different regions of the world

Because the technique used here for the investigation of the scaling properties of the high-frequency parts of the ground motion is virtually identical to those used in studies

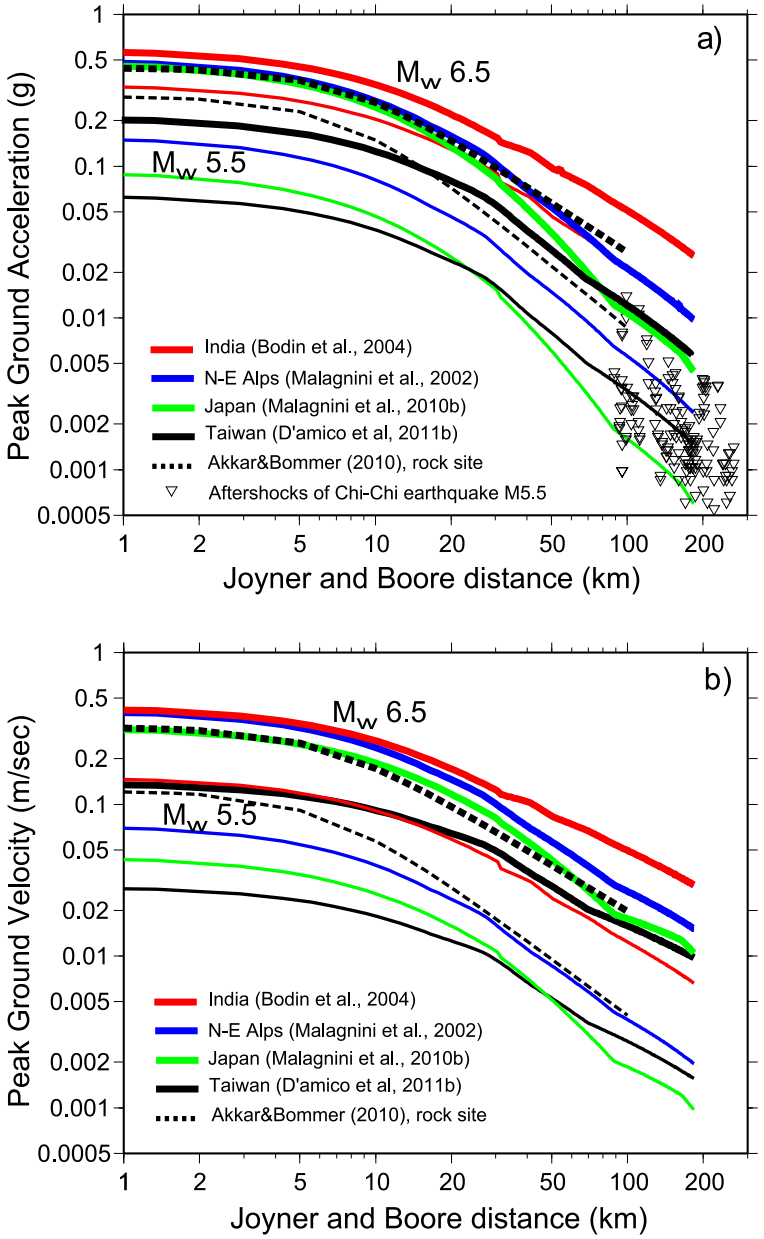

Fig. 7. Predictions of (a) PGA, in g and (b) PGV, in m/sec for different regions of the world: India (red lines, Bodin *et al* ., 2004); N-E Alps (blue lines, Malagnini *et al* ., 2002); Japan (green lines, Malagnini *et al* ., 2010b); Taiwan (black lines, this study). Predictions obtained using Akkar & Bommer (2010) are also shown by dashed black lines. The thick and thin lines are the prediction of PGA and PGV for moment magnitude of 5.5 and 6.5, respectively

conducted in a wide variety of environments (e.g., Bodin *et al*., 2004; Malagnini *et al*., 2010), we can compare our results with those studies to reveal systematic similarities and differences with other areas. Figure 7 shows the predicted ground motions computed for moment magnitude of $\mathbf{M_w}$ 6.5 and 5.5 from different regions of the world using the generic rock sites by Boore & Joyner (1997), and provide a comparison with the attenuation relationship developed by Akkar and Boommer (2010) (hereafter AB10).

For example in Figure 7 it is clear that weak-motion based predictive relationships fit quite well with the observed data from $\mathbf{M_w}$ 6.5 and 5.5 events in Taiwan. The predictive relationships of AB10 overestimate the PGA and PGV with compare to both our RVT-generated ground motion predictions and the observed data at lower magnitude, $\mathbf{M_w}$ 5.5. The predicted decay of PGA and PGV with distance clearly indicates that Taiwanese ground motions may be similar to that observed in tectonically active regions, rather than in stable

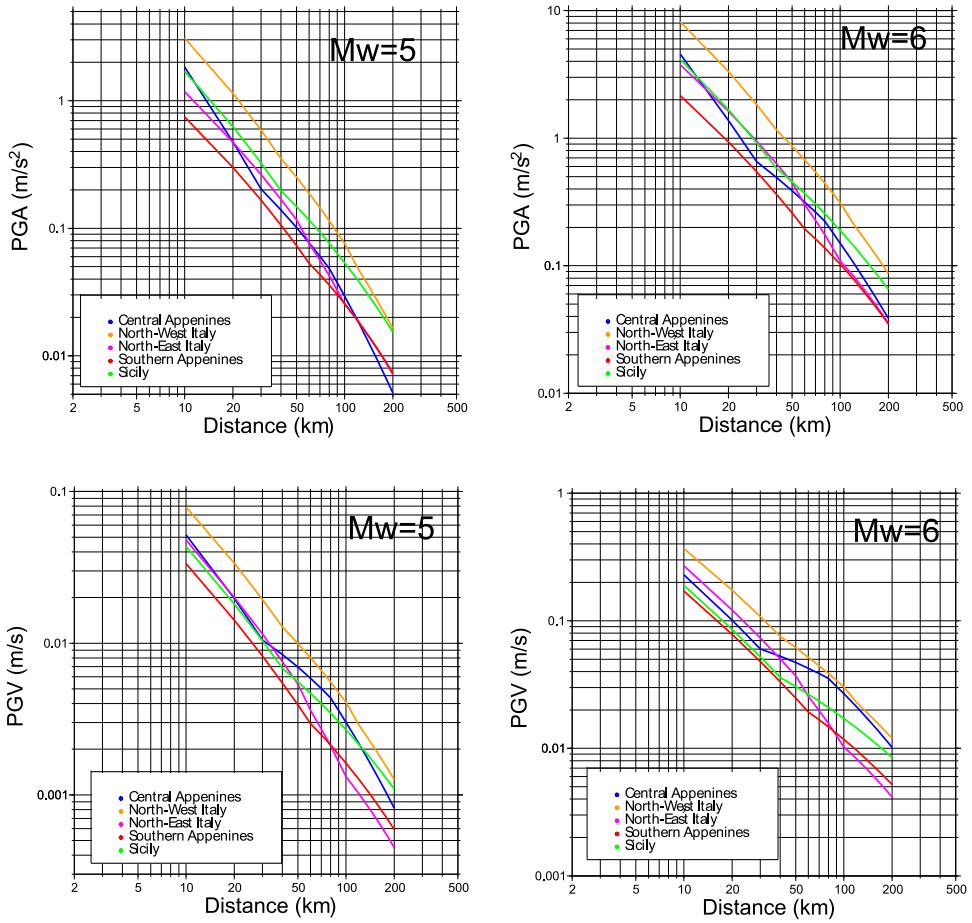

Fig. 8. Comparison of different estimates of PGA and PGV for different Italian regions as a function of moment magnitude Mw.

areas like the Indian plate. The differences in the predicted peak amplitudes between regions get larger at lower magnitudes. The stronger attenuation is experienced by the high-frequency part of the spectrum since peak ground motions are carried by a dominant frequency band that is magnitude-dependent. Most of the seismic energy is radiated around the earthquake corner frequency, so that at larger magnitudes, peak ground motions are dominated by lower frequencies and are not very sensitive to crustal attenuation. Therefore, peak ground motions decay faster for the $\mathbf{M_w}$ 5.5 event than for the $\mathbf{M_w}$ 6.5 event. Moreover, the level of ground shaking increases as the quality factor Q_o increases, and as the slope of the effective geometrical spreading function gets more gentle. The effect gets more severe for distant records. Due to the heterogeneities that are present (mainly vertically) in the crustal structure, different slopes may be presented in the predicted curves. Unfortunately, many of the existing predictive relationships (e.g., Ambraseys, 1995; Sabetta & Pugliese, 1996; Akkar & Bommer, 2010) were obtained by forcing a body-wave geometrical spreading to a distance range where supercritical reflections at the Moho appear to be quite important. Another important parameter is the stress drop, which may cause the differences in the ground motion levels at short distances and must be carefully calibrated in the region of interest. For example, Malagnini et al. (2010) observed that the absolute levels of the stress drop parameters are region-dependent that results in different estimation of gorund motion paramters. As an example, Figure 8 shows the comparison of simulated PGA and PGV as a function of distance for moment magnitude of 5 and 6 obtained using the SMSIM programs (Boore, 2003; http://www.daveboore.com/software_online.htm). It is clear how the predictions of the ground motion are different in the different areas, therefore the regional calibration of attenuation properties and source scaling is a really important task even considering a quite small area.

5. Conclusions

Such kind of studies clearly demonstrate that the weak-motion based ground-motion predictive equations successfully predict the ground motions induced by larger events, once the source term is adequately calibrated (D'Amico et al. 2011b; Malagnini *et al*., 2010).

The results obtained applying the technique described in this chapter could be used for upgrading the most recent hazard map of Italy and for engineering designs as well. The results are also useful to implement tools like *Shake Map*® (Wald et al. 2005) which use this kind of information to generate a rapid earthquake response. *ShakeMap*® is a tool used to portray the extent of potentially damaging shaking following an earthquake. It can be used for emergency response, loss estimation, and public information. Shake maps show the distribution of ground shaking in the region, information that can be really critical for emergency management decision making. In fact, it is the distribution of peak ground motion and intensity rather than the magnitude that provides useful information about areas prone to damage. Having this information in real time will result in lives saved and reduction in property damage. After a damaging earthquake, emergency managers must quickly find answers to important questions such as the localization of the most serious damage, and the areas with less; the resources that must be mobilized and in what quantity. Usually government response organizations answer these questions after a preliminary survey of the damaged area. This reconnaissance can require several hours or sometimes some days to be completed. As a result, decisions regarding search and rescue, medical emergency response, care and shelter for the damaged and displaced persons, and other

critical response needs must often be made while information is still incomplete. In this context a rapid and automatic response for the injured area is really important; hence predictive attenuation relationships play a key and really important role in similar tools.

6. Acknowledgements

This research was carried out using computational facilities procured through the European Regional Development Fund, Project ERDF-080 'A supercomputing laboratory for the University of Malta (http://www.um.edu.mt/research/scienceeng/erdf_080). Some of the figures were made using the Generic Mapping Tools (GMT) by Wessel and Smith (1991). The authors are also very thankful to Mr. Igor Babic and Ms Ivana Lorkovic for their support.

7. References

Aki, K., 1980. Attenuation of shear waves in the lithosphere for frequencies from 0.05 to 25 Hz, *Phys. Earth Planet. Inter*., 21, 50-60.

Akkar, S., & Bommer, J. J., 2010, Empirical equations for the prediction of PGA, PGV, and spectral accelerations in Europe, the Mediterranean, and the Middle East. *Seismological Research Letters* 81 (2), 195–206.

Akinci, A., Malagnini, L., Pino, N. A. , Scognamiglio, L., Hermann, R. B. & Eyidogan H. , 2001. High-frequency ground motion in the Erzincan region. Turkey: inferences from small earthquakes, *Bull. Seism. Soc. Am.* 91, 1446–1455.

Akinci A., Malagnini, L., Herrmann, R. B., Gok R., & Sorensen M. B., 2006. Ground motion scaling in Marmara region, Turkey. *Geophys. Journ Int*., 166, 635-651

Akinci, A., Malagnini, L., 2009. The 2009 Abruzzo earthquake, Italy. IRIS Newsletter, 1, 3.

Akinci, A., Malagnini, L. & Sabetta, F., 2010. Characteristics of the strong ground motions from the 6 April 2009 L'Aquila earthquake, Italy, *Soil Dyn. Earthq. Eng*., 30, 320-335, doi:10.1016/j.soildyn.2009.12.006

Ambraseys, N. N., 1995. The Prediction of Earthquake Peak Ground Acceleration in Europe, *Earthquake Engineering and Structural Dynamics*, 24, 467-490

Ambraseys, N. N., K. A. Simpson, and J. J. Bommer 1996. Prediction of horizontal response spectra in Europe, *Earthquake Eng. Struct. Dyn.* 25, 371–400

Ambraseys, N. N., and Simpson K. A., 1996. Prediction of vertical response spectra in Europe, Earthquake Eng. Struct. Dyn., 25, 401–412

Atkinson, G.M., & Silva, W. 1997. An empirical study of earthquake source spectra for California earthquakes. *Bull. Seism. Soc. Am*., 87, 97-113.

Azzaro, R. and Barbano, M.S., 2000. Analysis of the seismicity of Eastern Sicily: a proposed tectonic interpretation. Ann. Geofis. 43(1), 171 – 188

Bay, F., Fah, D., Malagnini, L., Giardini, D., 2003. Spectral shear-wave ground motion scaling for Switzerland, Bull. Seism. Soc. Am., 93, 414–429.

Beresnev I., & Atkinson G., 1998. FINSIM: a FORTRAN program for simulating stochastic acceleration time histories from finite faults, *Seism. Res. Lett*., 69, 27-32

Bodin, P., Malagnini, L. & Akinci A., 2004. Ground motion scaling in the Kachchh basin, India, deduced from aftershocks of the 2001 *M*w7.6 Bhuj earthquake, *Bull. Seism. Soc. Am.* 94, 1658–1669

Boore, D.M., 1996. SMSIM - Fortran programs for simulating ground motion from earthquakes: version 1.0, U.S. Geological Survey open-file report 96-80-A, 73 pp.

Boore, D.M., 2003. Simulation of ground motion using the stochastic method. *Pure and Applied Geophysics*, 160, 635-676

Boore, D. M., 2009. Comparing stochastic point-source and finite-source ground-motion simulations: SMSIM and EXSIM, *Bull. Seism. Soc. Am.* 99, 3202-3216

Boore, D. M. & Joyner, W. B., 1997. Site amplification for generic rock sites, *Bull. Seism. Soc. Am.* 87, 327-341.

Boore, D. M.,W. B. Joyner, and T. E. Fumal, 1993. Estimation of response spectra and peak acceleration from western North America earthquakes: an interim report, U.S. Geol. Surv. Open-File Rept. 93-509, 72 pp

Boore, D. M. & Atkinson, G. M., 2008. Ground-motion prediction equations for the average horizontal component of PGA, PGV, and 5%-damped PSA at spectral periods between 0.01 s and 10.0 s, *Earthquake Spectra* 24, 99-138.

Brune, J.N., 1970. Tectonic stress and the spectra of seismic shear waves from earthquakes. *J.Geophys. Res*., 75, 4997-5009.

Brune, J.N., 1971. Correction. J. *Geophys. Res*., 76, 5002.

Campbell, K. W., and Y. Bozorgnia (1994). Near-source attenuation of peak horizontal acceleration from worldwide accelerograms recorded from 1957 to 1993, in *Proc. Fifth U.S. National Conference on Earthquake Engineering*, EERI, Berkeley, California, Vol. 1, 283–292.

Campbell, K. W. & Bozorgnia, Y. , 2008. NGA ground motion model for the geometric mean horizontal component of PGA, PGV, PGD and 5%-damped linear elastic response spectra at periods ranging from 0.1 s to 10.0 s. *Earthquake Spectra,* 24 (1), 139–171.

Cartwright D.E., &Longuet-Higgins, M.S., 1956. The statistical distribution of the maxima of a random function, *Proc. R. Soc. London*, 237, 212-232.

Chouet B. K., & Tsujiurs M., 1978. Regional variation of the scaling law of earthquake source spectra. *Bull. Seism. Soc. Am.* 68, 49-79.

D' Amico, S.,K. D. Koper, R. B. Herrmann, A. Akinci, L. Malagnini, 2010a, Imaging the rupture of the Mw 6.3 April 6, 2009 L' Aquila, Italy earthquake using back-projection of teleseismic P-waves, Geophys. Res. Lett., 37, L03301, doi:10.1029/2009GL042156

D'Amico S., Orecchio B., Presti D., Zhu L., Herrmann R. B., Neri G., 2010b. Broadband waveform inversion of moderate earthquakes in the Messina straits, Southern Italy, Physics of Earth and Planetary Interiors, 179, 97-106, doi: 10.1016/j.pepi.2010.01.012

D'Amico S., Orecchio B., Presti D., Gervasi A., Guerra I., Neri G., Zhu L., Herrmann R. B., 2011a. Testing the stability of moment tensor solutions for small and moderate earthquakes in the Calabrian-Peloritan arc region. Boll. Geo. Teor. Appl. doi:10.4430/bgta0009 (in press)

D'Amico S., Akinci A., Malagnini L., 2011b. Predictions of high-freqeuncy ground-motion in Taiwan based on weak motion data, submitted to Geophysical Journal International

D'Amico S., Galea P., Borg P. R., Lotteri A., 2011c. Earthquake ground-motion scenario: case study for the Xemjia Bay (Malta) area. Proceedings of the International conference of Europen Council of Civil Engineers, 149-160

D'Amico S., Akinci A., Malagnini L., Herrmann R. B., 2011d. Ground motion scaling in southern Apennines (Italy). In preparation

Hanks, T.C. & Kanamori H., 1979. A moment magnitude scale. *J. Geophys. Res*., 84, B5, 2348-2350.

Herrmann, R. B., and Malagnini, L., 1996. Absolute ground motion scaling in the New Madrid Seismic Zone, Seism. Res. Lett. 67, 40.

Herrmann, R. B., and Dutt, J., 1999. High frequency vertical ground motion in the Pacific Northwest using PNSN data, Seism. Res. Lett. 70, 216

Hess, R. L., 2008, Unreinforced Masonry (URM) Buildings, in The ShakeOut Scenario, USGS Open File Report 2008-1150

Jeon Y.S., and Herrmann, R. B., 2004. High-frequency ground-motion scaling in Utah and Yellowstone. Bull. Seism. Soc. Am. 94, 1644-1657.

Kramer S.L. (1996). Geotechnical Earthquake Engineering. Prentice Hall, Upper Saddle River, NJ.

Ma, K.F., Mori, J., Lee, S.-J., & Yu, S.B., 2001. Spatial & temporal distribution of slip for the 1999 Chi-Chi, Taiwan, Earthquake, *Bull. Seism. Soc. Am.* 91, 1069–1087

Malagnini, L. & Herrmann, R.B., 2000. Ground motion scaling in the region of the Umbria-Marche earthquake of 1997, *Bull. seism. Soc. Am.*, 90,1041–1051.

Malagnini, L., Herrmann, R.B., & M. Di Bona 2000a. Ground motion scaling in the Apennines (Italy). *Bull. Seism. Soc. Am*., 90, 1062-1081.

Malagnini, L., Herrmann, R.B., & Koch, K., 2000b. Ground motion scaling in Central Europe, *Bull. Seism. Soc. Am*., 90, 1052-1061.

Malagnini, L., Akinci, A., Herrmann, R.B., Pino, N.A. & Scognamiglio, L, 2002. Characteristics of the ground motion in Northeastern Italy, *Bull. seism. Soc. Am.,* 92, 2186–2204.

Malagnini, L., Scognamiglio, L., Mercuri, A., Akinci, A. & Mayeda, K., 2008. Strong evidence for non-similar earthquake source scaling in central Italy, *Geophys. Res. Lett.,* 35, L17303, doi:10.1029/2008GL034310.

Malagnini, L., Nielsen, S., Mayeda, K. & Boschi, E., 2010. Energy radiation from intermediate to large magnitude earthquakes: implications for dynamic fault weakening, *J. geophys. Res.,* doi:10.1029/2009JB006786.

Malagnini, L., Akinci, A., Mayeda, K., Herrmann, R.B. & Munafo', I., 2010b. Accurate predictions of strong ground motion based on weak motion data: case studies from Italy and Japan, in *Proceedings of the 2010 SSA Annual Meeting*, Portland, OR, 21–23 April 2010

Morasca, P., Malagnini, L., Akinci, A., Spallarossa, D., Herrmann, R.B., 2006. Ground motion scaling in the western Alps. J. Seismol., 10, 315-333.

Motezedian, D., & Atkinson, G. M., 2005. Stochastic finite-fault modeling based on a dynamic corner frequency, *Bull. Seism. Soc. Am.* 95, 995-1010.

Ortega, R., Herrmann, R. B., Quintanar L., 2003. Earthquake ground-motion scaling in Central Mexico between 0.7 and 7 Hz, Bull. Seism. Soc. Am. 93, 397–413

Panzera F., D'Amico S., Galea P., Lombardo G., Pace S., 2011. Vs30 estimates in Malta. In preparation

Pino, N. A., Malagnini, L., Akinci, A., Scognamiglio, L., Herrmann, R. B., Stavrakakis, G., Chouliaras, G., 2001. Ground motion scaling relationships for mainland Greece and Crete, Seism. Res. Lett. 72, 258.

Raoof, M., Herrmann, R.B. & Malagnini, L., 1999. Attenuation and excitation of three component ground motion in Southern California, *Bull. Seism. Soc. Am.* 89, 888-902

Rapolla A., Akinci A., Bruno P. P., D'Amico S., Di Fiore V., Malagnini L., Maschio L., Paoletti V., Secomandi M., Vietri A., 2008. La pericolosità sismica: dalla classificazione sismica alla microzonazione dei territori comunali, alla risposta sismica del sito. Liguori Editore

Sabetta, F., and Pugliese A., 1987. Attenuation of peak horizontal acceleration and velocity from Italian strong-motion records, Bull. Seism. Soc. Am. 77, 1491–1511.

Sabetta, F., and Pugliese A. 1996. Estimation of response spectra and simulation of nonstationary earthquake ground motion, Bull. Seism. Soc. Am. 86, 337–352.

Scognamiglio, L., Malagnini, L., Akinci, A., 2005. Ground motion scaling in eastern Sicily, Italy. Bull. Seism. Soc. Am. 95, 568-578

Wald, D., Worden, B., Quitoriano, V., Pankow, K. L., 2005. Shake Map manual: technical manual, user's guide, and software guide. U.S. Geological Survey Techiniques and Methods, book 12, section A, 132 pp.

Wells, D. L., and Coppersmith K. J., 1994. New empirical relationships among magnitude, rupture length, rupture width, rupture area, and surface displacement, Bull. Seism. Soc. Am. 84, 974–1002.

Wessel, P. & Smith, W. H. F., 1991. Free software helps map and display data, *Eos Trans.*, AGU, 72, 441